Received: 6 August 2021 | Accepted: 1 May 2022

DOI: 10.1002/bab.2367

ORIGINAL ARTICLE

WILEY

Recombinant human carbonic anhydrase VII: Purification, characterization, inhibition, and molecular docking studies

Hatice Esra Duran[1] | **Şükrü Beydemir**[2,3]

[1]Department of Medical Biochemistry, Faculty of Medicine, Kafkas University, Kars, Turkey

[2]Department of Biochemistry, Faculty of Pharmacy, Anadolu University, Eskişehir, Turkey

[3]The Rectorate of Bilecik Şeyh Edebali University, Bilecik, Turkey

Correspondence
Şükrü Beydemir, Department of Biochemistry, Faculty of Pharmacy, Anadolu University, 26470, Eskişehir, Turkey.
E-mail: sukrubeydemir@anadolu.edu.tr

Abstract

Human carbonic anhydrase VII (*h*CA VII), a cytosolic enzyme, defends against oxidative stress by preventing reactive oxygen species from forming. In our study, first, *h*CA VII was cloned into *Escherichia coli* (One Shot Mach1-T1R) strain by using cDNA of the human brain and successfully expressed. The integrity of the plasmid generated by colony PCR was checked, and after, for protein expression, the plasmid was transformed into *E. coli* BL21 (DE-3) strain. hCA VII expression was observed after 6 h of isopropyl-D-1-thiogalactopyranoside (IPTG) induction. The fusion protein containing hexahistidine (6xHis) was purified with 7.02 EU/mg of specific activity, had 48.07% of purification yield, and approximately 21-folds using a ProbondTM nickel chelating resin affinity column. Then, both molecular mass determination and purity control of the purified recombinant enzyme was done by SDS-PAGE (sodium dodecyl sulfate-polyacrylamide gel electrophoresis). The mass of the SUMO-*h*CA VII fusion protein was calculated as 46.77 kDa. As a result of Western blot analysis using anti-His G-HRP antibody, the fusion protein was detected as approximately 45 kDa. Furthermore, the characterization assays and in vitro inhibition studies were done for the recombinant enzyme. K_I values of these agents were found between 0.29 μM and 157.6 mM. Finally, molecular docking investigations of these antibiotics were undertaken to understand further the binding interactions on the active site of this recombinant enzyme.

KEYWORDS

carbonic anhydrase, *E. coli*, enzyme catalysis, metalloenzymes, molecular docking, recombinant protein

1 | INTRODUCTION

Today, a new era is approaching due to the increase in the level of knowledge in medicine, genetics, and proteins in solving the functioning mechanisms of various diseases and making the correct diagnosis and necessary treatment approaches. It has been put into practice by scientists for many years. Many human proteins such as antibodies, vaccines, natural interferons, and various metabolic enzymes have been recombinantly produced to diagnose and treat many diseases. These products are used in many fields, especially medicine.[1] Carbonic anhydrase (CA; E.C.4.2.1.1) enzyme, is coordinated with either iron, cadmium, or zinc through three histidine residues in its active site, is a

Abbreviations: CA, carbonic anhydrase; *h*CA VII, human carbonic anhydrase VII; OD, optic density; r*h*CA VII, recombinant human carbonic anhydrase VII; SDS-PAGE, sodium dodecyl sulfate-polyacrylamide gel electrophoresis.

metalloenzyme. CA catalyzes the transformation of CO_2 and HCO_3^-.[2] CAs are present in bacteria, archaea, and eukarya.[3] According to their structural similarities, CAs are classified as alpha (α), beta (β), gamma (γ), epsilon (ε), delta (δ), zeta (ζ), eta (η), and theta (θ). Among these classes, the α-class CAs studied in detail are mammals, fungi, prokaryotes, plant cytoplasm, protozoa, and algae.[4] Zinc-dependent metalloenzymes play different roles in diverse organisms. Some of these are for the transportation of CO_2 and HCO_3^-, respiration, and CO_2–pH balance.[5,6]

The amino acid sequences of CA gene families are not similar. α-CAs are the class of CA found in humans, of the 16 human α-CA isoforms, cytosolic ones: CA I-III-VII-XII; membrane-bound ones: CA IV-IX-XII-XIV-XV; mitochondrial ones: CA VA-VB; and secretory: CA VI.[7] CAs contain zinc ions (Zn^{2+}) in their active site. This is necessary for CA to be active. Many studies have been done to understand the inhibition and activation of CA enzymes. Substances such as sulfamides, sulfonamides, many inorganic anions, and sulfamates cause the enzyme to be inhibited.[8,9] Inhibition of CAs has a significant function in treating many illnesses such as diabetes, epilepsy, and cancer.[10] Therefore, CA inhibitors are frequently used in medicine.[11–13] Human carbonic anhydrase VII (*h*CA VII) protects against oxidative stress by inhibiting the formation of reactive oxygen species.[14,15] *h*CA VII, a cytosolic enzyme, is also expressed in the salivary glands and hippocampus. However, its distribution in different tissues is not known. *h*CA VII gene is localized on chromosome 16q21-23.[16] The *h*CA VII gene is thought to be involved in the mechanism of GABAergic excitement and seizure generation.[17] Furthermore, its role controlling neuropathic pain has recently been hypothesized; however, the mechanism is unknown.[18]

Antibiotics are extensively used in human therapy to prevent and cure illnesses and promote growth.[19] In addition, antibiotics play an important role in combating bacterial infections.[20] The term antibiotics is defined in medicine as compounds that can be natural or synthetic that neutralize microorganisms. Antibiotics must be targeted to the microorganism in order to have a beneficial effect. Therefore, the main target of antibiotics is bacterial cell walls. Antibiotics show their effects on bacterial cell properties or mechanisms. For example, β-lactams and glycopeptides inhibit cell wall synthesis, aminoglycosides and tetracyclines cause protein synthesis inhibition, and fluoroquinolones and rifamycins cause nucleic acid inhibition.[21]

Because CAs are found in many tissues and in distinct isoforms, scientists have been able to build inhibitors with biomedical uses. In clinical practice, enzyme inhibitors are frequently utilized. Our study aims to produce a fast and simple recombinant *h*CA VII (r*h*CA VII) enzyme and to understand the biochemical behavior of the enzyme against therapeutics. For this purpose, we have conducted an investigation involving cloning, expression, purification, characterization, and inhibition of r*h*CA VII. We have also carried out molecular docking studies to assess commonly used antibiotics' inhibition mechanisms against r*h*CA VII.

2 | EXPERIMENTAL

2.1 | Materials

We used human brain cDNA from Clontec, pET-SUMO vector from Invitrogen, p-nitrophenolate, GeneJET Plasmid Miniprep, Triton X-100, NaCl, guanidine hydrochloride, imidazole, NaH_2PO_4, and glycerol from Sigma, protein molecular weight marker from Thermo, and the IPTG from BBI Fermentas. Metabion synthesized forward primer and reverse primer.

2.2 | Cloning of *h*CA VII using the pET-SUMO vector

First, with reverse primer (5-AAGGAGGCCTTTACCAC-3) and forward primer (5-ATTGGCACAAGCTGTATCCC-3), *h*CA VII was generated from the human brain cDNA by PCR method. PCR was performed as follows: 4 min at 94°C, 35 cycles (1 min at 94°C, 30 s at 51.5°C, 1 min at 72°C) and finally 5 min at 72°C. The purity control for the PCR result was made by agarose gel electrophoresis. The binding of the pET-SUMO vector with the *h*CA VII gene from the His6 region in the N-terminal region occurred. It was left to ligation overnight at 16°C. After ligation, the plasmid containing the *h*CA VII gene was transferred to *Escherichia coli* One-Shot Mach1-T1R cells. The cells were incubated overnight at 37°C in the plate containing LB kanamycin. Colonies incubated overnight were grown in LB after harvesting. The obtained pET-SUMO-r*h*CA VII was isolated with GeneJET Plasmid Miniprep. Later, sequence analysis was done at Iontek Company.

2.3 | Expression of *h*CA VII gene

After sequence analysis, the plasmid for protein expression was transformed into *E. coli* BL21 (DE-3) strain. Bacteria were grown at 37°C in LB supplemented with 1 mg/ml kanamycin. When the optic density (OD) was 0.8, at 600 nm, the bacteria were transferred to LB with 1 mg/ml kanamycin and grown at 225 rpm and 37°C. Then when OD 600 was 0.8, the gene was induced with IPTG

TABLE 1 PCR product sizes for different combinations

Reaction	F. primer	R. primer	Size (bp)
1	Gene	Gene	794
2	Vector	Gene	899
3	Gen	Vector	947
4	Vector	Vector	1052

(0.5 mM) for 6 h. The cells we obtained were centrifuged. After centrifugation, the pellet was resuspended in the lysis buffer. Cells were incubated on ice by adding lysozyme. Obtained lysis was centrifuged at 5000 rpm for 15 min. The sodium dodecyl sulfate-polyacrylamide gel electrophoresis (SDS-PAGE) gel electrophoresis was performed for purity analysis.

2.4 | Purification of *h*CA VII

Lysozyme, DTT, and glycerol were added to the lysate, and the sample was incubated on ice. Pellets were split using a sonicator. After adding 0.1% Triton X-100, the sample was shaken for 2–3 hours. After the sample was centrifuged, the clear lysate was loaded into 2 ml of Ni-NTA resin. The lysate was passed through the column, and then first 25 ml of buffer I, then 25 ml of buffer II, were passed from the column. Buffer III was used for washing the column. Finally, 10 ml of elution buffer was used to elute the recombinant protein attached to the column. The fractions collected in elution were dialyzed twice in dialysis buffer for 2 h at 4°C. Quantitative protein determination, Western blot, SDS-PAGE electrophoresis, enzyme activity measurement, and inhibition studies were performed in the sample obtained after dialysis. The molecular docking study was performed according to the inhibition result obtained.

2.5 | Protein analysis

Qualitative protein determination was done by the Bradford method.[22–24] The purity analysis and molecular mass determination of the recombinant protein were performed according to the Laemmli method.[25–27] The size of the fusion protein was determined by Western blot analysis.

2.6 | r*h*CA VII activity assay

r*h*CA activity was determined by using the esterase activity.[28,29]

2.7 | Characterization study for r*h*CA VII

Determination of optimum pH, optimum temperature, ionic intensity, activation energy, activation enthalpy, Q10 value, K_M, and V_{max} values for rhCA VII was carried out as per the protocols elucidated in the previous studies by our group.[30–32]

2.8 | In vitro inhibition study

The inhibition effects of antibiotics on recombinant enzyme were investigated using five different inhibitor concentrations. Control cuvette had enzyme activity only, but no inhibitor was added. The IC_{50} value was accepted as the inhibitor concentration causing 50% inhibition and this value for each inhibitor was calculated graphically.[33–36] The inhibition types and K_I constants were found by Lineweaver–Burk's curves[37,38] as described in previous studies.[39–42] Analysis of the data was realized using GraphPad Prism version 8 for Mac (GraphPad Software, La Jolla, CA, USA). Differences between datasets were considered statistically significant when the *p*-value was less than 0.05.

2.9 | Molecular docking study

The molecular docking analysis was performed within the Schrödinger Small-Molecule Drug Discovery Suite 2021-1 for Mac (Schrödinger, LLC, NY, USA) using

TABLE 2 Summary of SUMO-*h*CA VII fusion protein by affinity column r*h*CA VII purification from inclusion body in denaturating conditions and refolding

Purification steps	Activity (EU/ml)	Total volume (ml)	Protein (mg/ml)	Total protein (mg)	Total activity (EU)	Specific activity (EU/mg)	Yield (%)	Purification fold
Lysate	0.84	8	2.52	20.16	6.72	0.33	100	1
SUMO-*h*CA VII purified from Ni resin affinity column	3.23	1	0.46	0.46	3.23	7.02	48.07	21.07

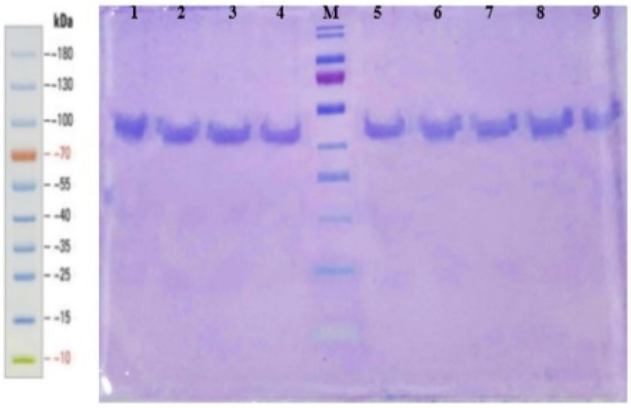

FIG 1 Sodium dodecyl sulfate-polyacrylamide gel electrophoresis (SDS-PAGE) analysis of pET-SUMO-r*h*CA VII (M: marker, 1-2-3-4-5-6-7-8-9; purified pET-SUMO-*h*CA VII)

the panels: Maestro,[43] Protein Preparation Wizard,[44] SiteMap,[45] Receptor Grid Generation,[46] LigPrep,[47] and Prime MM-GBSA.[48] First, the crystal structure of *h*CA VII (PDB ID: 6H37; species: Homo sapiens; resolution: 1.90 Å; *R*-values free and work: 0.236 and 0.194, respectively)[49] was downloaded from the Protein Data Bank.[50,51] The 6H37 was minimized using the Protein Preparation Wizard tool[52,53] applying force field OPLS4[54,55] with default parameters at pH 7.4 ± 0.5.[56,57] The active sites were predicted using the SiteMap module.[58,59] The grid was generated used the Receptor Grid Generation tool[60,61] with all the active site residues. Next, the 2D SDF format of all the drugs was sketched using ChemDraw version 19.1 for Mac (PerkinElmer, Inc., Waltham, MA, USA)[62,63] and converted into the 3D format using LigPrep module[64–66] with the OPLS4 force field. A one-step docking methodology was used, Glide XP.[67–69] Finally, MM-GBSA binding energies,[70–72] which estimate relative binding affinities for rifamycin, kanamycin, and lincomycin that exhibit competitive inhibition, were calculated in the OPLS4 force field and VSGB energy model.[73–75]

3 | RESULTS AND DISCUSSION

Recombinant DNA technology is a technology that is not possible to form spontaneously in nature, and involves the cutting of DNA molecules obtained from different biological species by genetic engineering technology and combining the different DNA parts obtained. In the past centuries, the development of the desired characteristics of living things by controlling the expression of the relevant gene was completely an imagination. However, the recombinant DNA technology that has developed in recent years allows this. The recombinant production of proteins that are associated with problems threatening human life has significantly increased the popularity of this technology in recent years. This technology, which focuses on the necessary improvements for human health, improvement of nutritional facilities, and reduction of the negative effects of the environment, is multidisciplinary. Recombinant technology makes it easy to reach the product safely and quickly in the health sector. Additionally, recombinant DNA technology, genetic modification, and gene therapy techniques are also widely used for the cure of biological reproduction and critical diseases.[76]

Cloning and expression are performed using the pET-SUMO vector. SUMO proteins can be synthesized in a precursor form prior to conjugation to the target protein, such as ubiquitins.[77] Cellular processes such as nuclear transport, transcriptional regulation, and protein stability on the SUMO-targeted protein are the main differences between these two groups.[78] One of the crucial problems encountered, especially in low-level hosts such as *E. coli*, is inefficient production of recombinant protein and soluble form. Approaches such as fusion proteins, promoter alteration, and chaperone co-expression are generally preferred to avoid this problem. In addition to providing expression and uniform folding of the target protein, the fusion proteins protect the protein of interest from degradation and facilitate purification and detection. For this reason, it has started to be preferred quite frequently in recombinant production techniques.[79]

Cellular metabolism involves the necessary series of reactions that allow movements. These series of reactions occurring in cells are defined as metabolic pathways. These metabolic pathways in living organisms form the metabolic network. Failure in occurrence of any of these pathways that make up the metabolic network can affect the entire metabolism. Almost all of the reactions in metabolism are carried out by catalysts called enzymes for fast and effective reactions. Therefore, the deficiency in enzymes or the activation–inhibition of the enzyme has the power to affect the whole metabolism. This situation reveals the importance of the enzyme–drug interaction. The mechanisms of action of drugs and chemicals can be understood by examining the activities of enzymes in metabolism.[80]

In this study, the recombinant vector was formed by applying the steps described in the method section. After the gene sequence was amplified (Figure S1), the protein was cloned into the pET-SUMO vector. The results of colony PCR (Figure S2), plasmid isolation, and cross-PCR (Figure S3) showed that the protein gene was correctly linked to the vector. The product length obtained was within the desired range (Table 1). The recombinant hCA VII protein was expressed in *E. coli*. The recombinant protein was produced using BL21 (DE3).

Electrophoresis for purity analysis was performed on the protein obtained after induction with IPTG. At the same time, the molecular mass was determined by SDS-PAGE. As a result, approximately 47.77 kDa fusion protein was obtained in pure form (Figure S4). The Bradford method's qualitative protein determination results are given in Table 2. The results show that induction by isopropyl-β-D-thiogalactopyranoside (IPTC) significantly affects the amount of protein (Figure 1). The recombinant protein was verified by applying Western blot analysis. The fusion protein mass was determined to be 45 kDa as expected (Figure S5).

Characterization studies were carried out on the recombinant enzyme. The optimum pH value of *r*hCA VII was assigned as pH 8.0 in Tris-H_2SO_4 buffer as the maximum activity was observed (Figure S6). As the study was performed to determine the ionic strength using a Tris-H_2SO_4 buffer between 0.1 and 1 M and 0.8 M Tris-H_2SO_4 buffer, pH 8.0 was determined as the ionic strength value of the recombinant enzyme (Figure S7). Determining the optimum temperature value of the r*h*CA VII due to the enzyme activity measurements between 0°C and 50°C, the highest enzyme activity was measured at 50°C (Figure S8). The Arrhenius curve calculated E_a, ΔH, and Q10 values. The results are as shown in Figure S9: E_a: 1843 kcal/mol, ΔH: 1199 kcal/mol, and Q10: 1.4 (Figure S9). Lineweaver–Burk plot was drawn with PNF used in different concentrations, and using the graph drawn, the K_M value was calculated as 1.36 mM and the V_{max} value as 0.405 EU/ml (Figure S10). The inhibitory effects of some antibiotics on r*h*CA VII enzyme activity produced and purified by bacteria were investigated under in vitro conditions. All the results obtained in the study are summarized in Table 3. IC_{50} curve and K_I graph for rifamycin sodium are given in Figures S11 and S12, respectively.

In our study, Lineweaver–Burk graphics were used to determine K_I constants and inhibition types for antibiotics showing inhibition effect on r*h*CA VII.[37] In order to obtain accurate results, $1/V$ and $1/[S]$ values were obtained at three different constant inhibitor concentrations for each inhibitor study. The IC_{50} value is defined as the concentration of inhibitor that halves enzyme activity. In our inhibition studies on r*h*CA VII enzyme activity, IC_{50} values were determined for each inhibitor, and the highest inhibition showed rifamycin sodium with an IC_{50} of 0.56 μM. This compound is followed by vancomycin HCl and tobramycin compounds with IC_{50} values of 51 and 59 μM, respectively. r*h*CA VII enzyme activity of the inhibitors studied in the order of magnitude from the following are as follows: rifamycin sodium > vancomycin HCl > tobramycin > amoxicillin > kanamycin sulfate > teicoplanin > gentamicin sulfate > amikacin sulfate > piperacillin sodium > cefuroxime sodium > clindamycin phosphate > lincomycin HCl > ampicillin sodium > cephazolin sodium > cephazolin sodium > cephazoline sodium. Among the compounds studied, it can be concluded that rifamycin sodium is a potent inhibitor of r*h*CA VII. According to the results of our inhibition studies, rifamycin sodium showed a high inhibition effect on r*h*CA VII enzyme. From the study, we infer that hydroxyl and methyl groups present in rifamycin sodium provide effective inhibition. Although the chemical structures of amoxicillin and ampicillin drugs were completely identical except for a single hydroxyl ion, we observed that the inhibition rates were quite different. Compared to IC_{50} values, amoxicillin showed a 231 times more inhibitory effect than ampicillin. In this case, it was concluded that the hydroxyl ion provides an effective inhibition of the enzyme r*h*CA VII.

When the cephalosporin group was compared in itself, cefaperazone sodium had the best inhibition effect compared to other antibiotics in the group (K_I: 0.304 mM). This can be explained by the fact that it contains hydroxyl ions in the structure, as mentioned above. Antibiotics of the fluoroquinone class (ciprofloxacin, levofloxacin, ofloxacin, and moxifloxacin) showed no inhibitory effect on the r*h*CA VII enzyme. The aminoglycoside class of antibiotics contains hydroxyl and amino groups. This class was effective in inhibiting the r*h*CA VII enzyme except for antibiotic netilmicin. Lincomycin HCl and clindamycin phosphate found in the class of lincosamides showed a more inhibitory effect than clindamycin phosphate (K_I: 1.80 mM). The fact that this antibiotic contained a chlorine atom changed the inhibition rate by about 5.3 times. In antistaphylococcal antibiotics, vancomycin HCl exhibited 11 times more effective inhibition than teicoplanin. This can be attributed to the fact that it contains an extra chlorine atom than teicoplanin. Accordingly, we can conclude that the enzyme r*h*CA VII is susceptible to chlorine, amino, and hydroxyl groups and that molecules containing these groups freely may be potential inhibitors of the enzyme r*h*CA VII.

Recent studies have shown that the identification of CA inhibitors is of tremendous value in understanding the roles of normal and disease processes. This has encouraged studies of the synthesis of more potent CA inhibitors. Therefore, today many researchers are developing strong and specific CA inhibitors.[81] Studies on the interaction of different enzymes purified from different sources with antibiotics increase day by day. For example, in 2009, the effect of antibiotics on the PON1 enzyme purified from human serum was examined. The order of antibiotics from small to large according to K_I values: teicoplanin > rifamycin > tobramycin > ceftriaxone sodium > cefuroxime sodium > ceftazidime pentahydrate > ornidazole > amikacin sulfate.[82] In another study, the effects of some

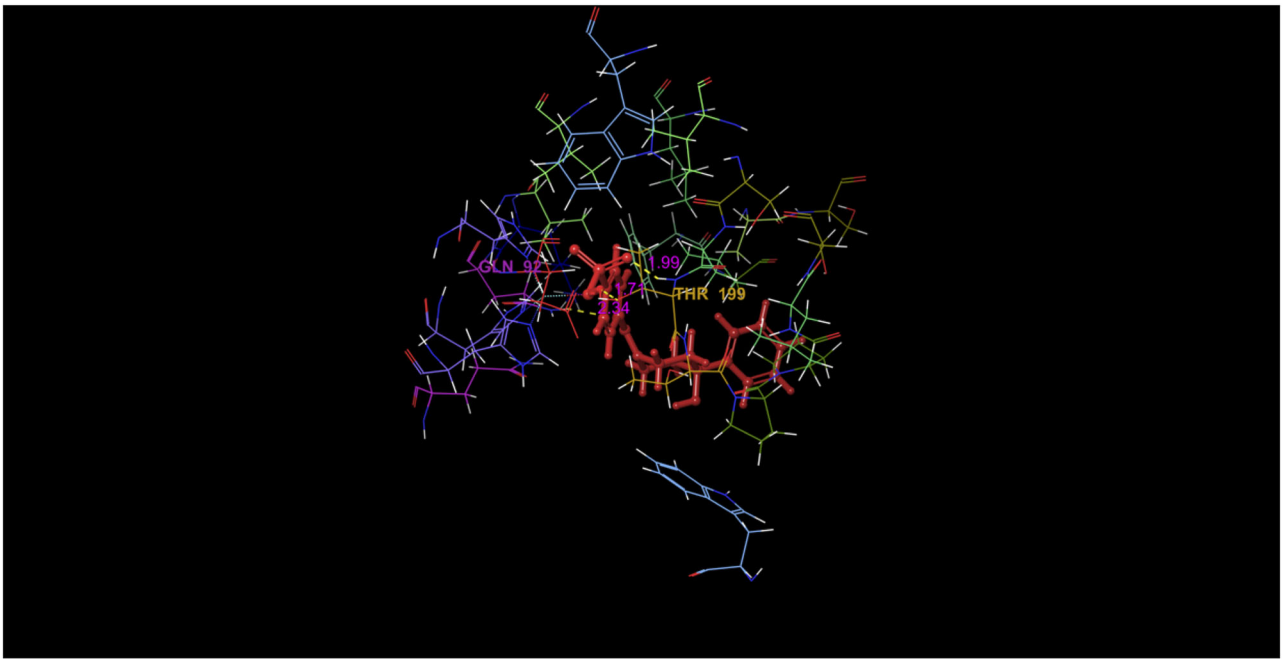

(A)

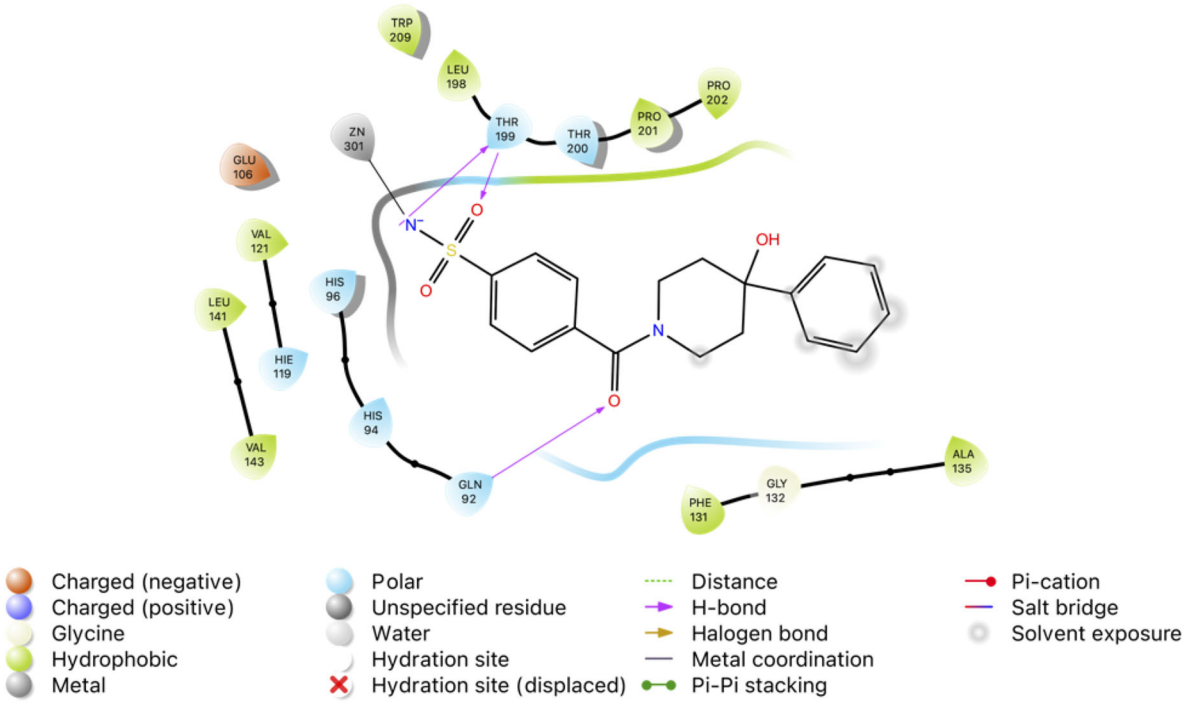

(B)

FIG 2 Molecular docking of *h*CA VII (PDB ID: 6H37) with native ligand FKQ (4-(4-oxidanyl-4-phenyl-piperidin-1-yl)carbonylbenzenesulfonamide). (A) 3D ligand interaction diagram of 6H37 with FKQ. (B) 2D docking pose of FKQ with the key amino acids within the binding pocket of 6H37

TABLE 3 IC_{50}, K_I values, and inhibition types for r*h*CA VII

Antibiotics	IC_{50} (mM)	K_I (mM)	Inhibition type
Rifamycin sodium	0.56[a]	0.29[a]	Competitive
Amoxicillin	60.00[a]	0.60[a]	Uncompetitive
Tobramycin	0.06	0.01	Uncompetitive
Kanamycin sulfate	0.08	0.03	Competitive
Vancomycin HCl	0.05	0.08	Noncompetitive
Cefoperazone sodium	0.48	0.30	Uncompetitive
Gentamicin sulfate	3.52	0.73	Uncompetitive
Teicoplanin	0.61	0.89	Noncompetitive
Clindamycin phosphate	7.62	1.80	Uncompetitive
Cefazolin sodium	34.65	4.95	Uncompetitive
Cefuroxime sodium	5.06	5.34	Uncompetitive
Piperacillin sodium	4.23	7.78	Noncompetitive
Amikacin sulfate	3.96	8.27	Noncompetitive
Ampicillin sodium	13.86	8.46	Uncompetitive
Lincomycin HCl	8.25	9.52	Competitive
Ceftriaxone sodium	53.32	157.60	Noncompetitive
Ciprofloxacin	NA	NA	–
Levofloxacin	NA	NA	–
Metronidazole	NA	NA	–
Moxifloxacin	NA	NA	–
Netilmicin	NA	NA	–
Ofloxacin	NA	NA	–
Ornidazole	NA	NA	–

Abbreviation: NA, not activated.
[a]μM.

antibiotics on *h*CA I and *h*CA II isoenzymes were examined in vitro. These examined antibiotics were found to inhibit *h*CAI and *h*CA II isoenzymes at a very low rate.[83] In another study examining the effects of antibiotics on enzymes, the inhibitory effects of cefoperazone, cefazolin, cefuroxime, ceftazidime, and ceftriaxone antibiotics on sheep kidney purified aldose reductase (AR) and sorbitol dehydrogenase (SDH) enzymes were investigated. While AR enzyme was inhibited by the drugs studied, SDH enzyme was inhibited only by cefuroxime.[84] The effect of antibiotics (gentamicin, amikacin sulfate, lincomycin, kanamycin sulfate, and clindamycin) on ALDH (alcohol dehydrogenase) enzyme purified from sheep liver was investigated in another study. IC_{50} values of these antibiotics were 43.31, 36.47, 20.38, 18.73, and 1.31 mM, respectively. Clindamycin was the antibiotic that showed the best inhibitory effect.[85]

First, to better understand the interactions of the drugs that exhibit competitive inhibition with 6H37, the rifamycin sodium, kanamycin sulfate, and vancomycin HCl were docked in the enzyme's binding site. For the re-docking computes, the structure of crystal ligand, including, FKQ (4-[4-oxidanyl-4-phenylpiperidin-1-yl]carbonylbenzenesulfonamide, PubChem Ref.: 135393500) in the active site, were used. The docked pose of FKQ overlapped with the pose in the X-ray crystal structure at a root mean square deviation value of 0.34. Next, in the present docking study, the docking pattern of FKQ (MM-GBSA value of −29.49 kcal/mol, docking score of −8.17 kcal/mol) was compared with that of these drugs, and the binding interactions of the inhibitors with the *h*CA VII are displayed in Figure 2.

An MM-GBSA value of −16.19 kcal/mol and docking score of −1.51 kcal/mol indicated that rifamycin is a tight binder for *h*CA VII. The -OH groups and carboxy moiety formed H-bond with residues His64 (distance 2.60 Å), Gln67 (distance 2.22 Å), Gln92 (distance 2.41 Å), and Asn62 (distance 1.87 Å), respectively. However, hydrophobic interactions were monitored between rifamycin and residues Trp5, Tyr7, Val121, Phe131, Ala135, Leu141, Val143, Leu198, Pro201, and Pro202 (Figure 3). Structurally, there was a relative correlation between the number of H-bonds and the MM-GBSA value. Accordingly, kanamycin (MM-GBSA value of −22.68 kcal/mol and docking score of −6.85 kcal/mol) formed six H-bond interactions between -OH groups and residues Trp5 (distance 1.83 Å), Asn62

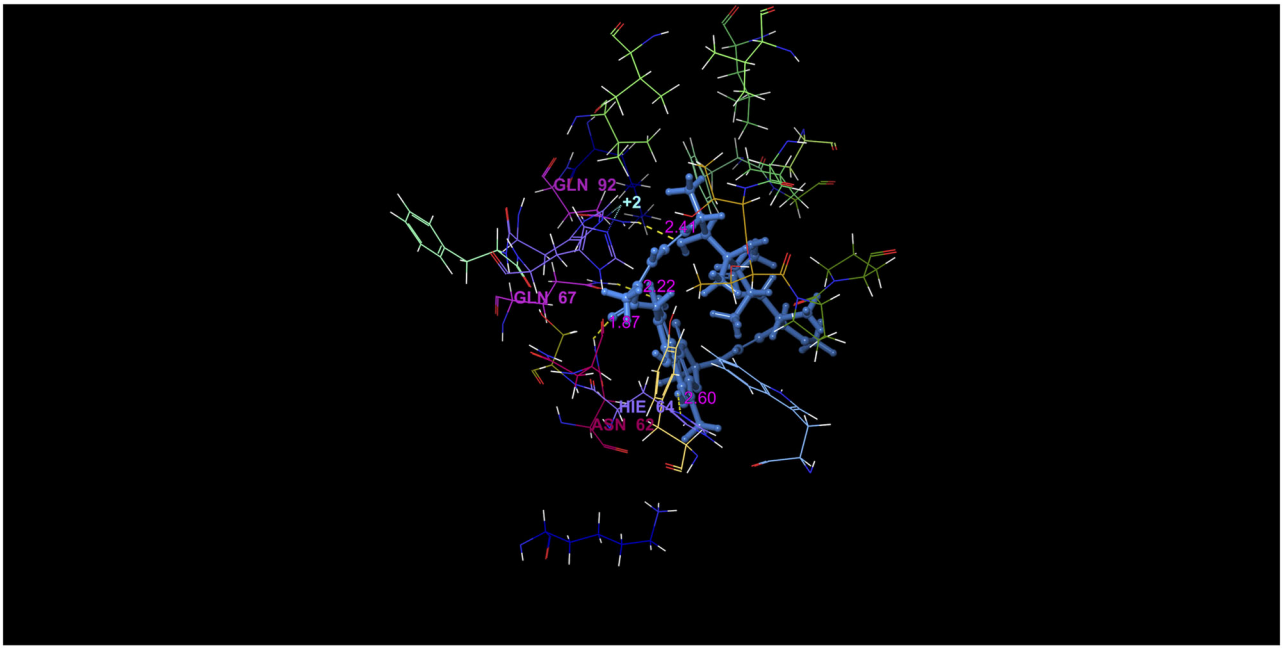

(A)

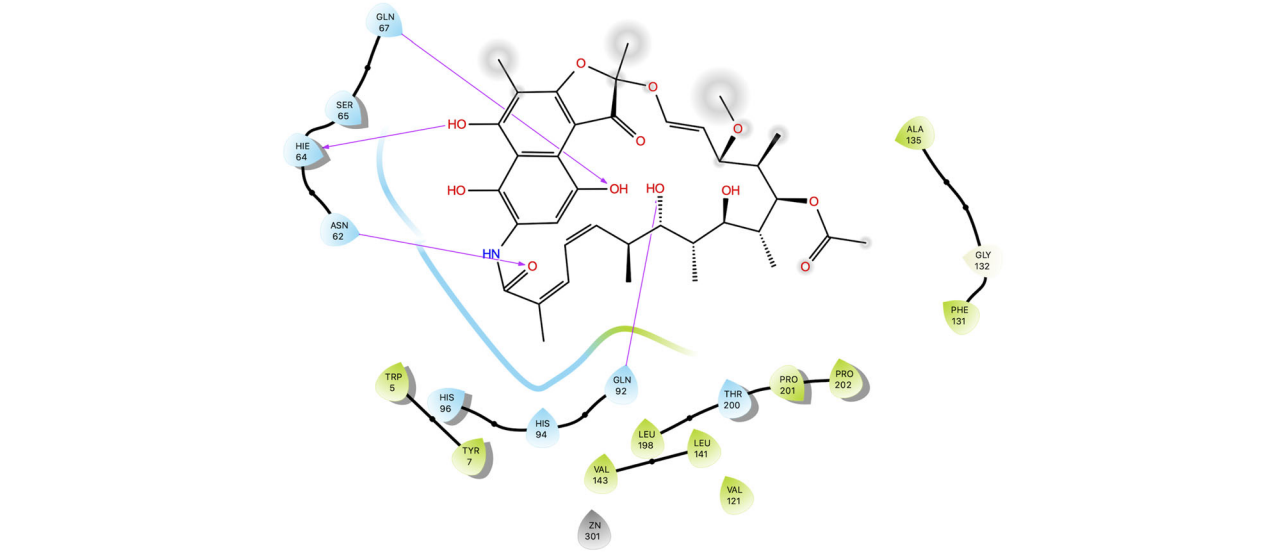

(B)

FIG 3 Molecular docking of *h*CA VII (PDB ID: 6H37) with rifamycin. (A) 3D ligand interaction diagram of 6H37 with rifamycin. (B) 2D docking pose of rifamycin with the key amino acids within the binding pocket of 6H37

(distance 2.54 Å), His64 (distance 2.31 Å), Gln67 (distance 1.78 Å), Gln92 (distance 2.10 Å), and Thr200 (distance 1.69 Å) of *h*CA VII, while amino moiety displayed Pi-cation interaction with His94. Nevertheless, kanamycin has hydrophobic fragments, Tyr20, Val121, Leu198, Pro201, and Pro202 (Figure 4). The docking showed that lincomycin (MM-GBSA value of −20.56 kcal/mol and docking score of −6.36 kcal/mol) has two H-bonds with Gln67 (distance

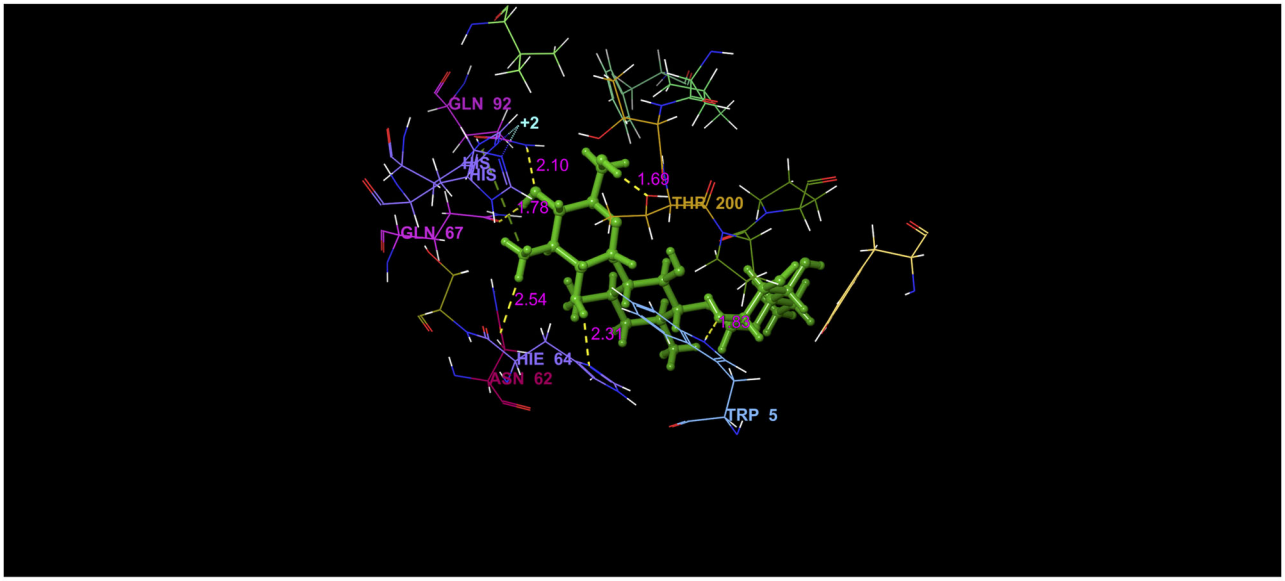

(A)

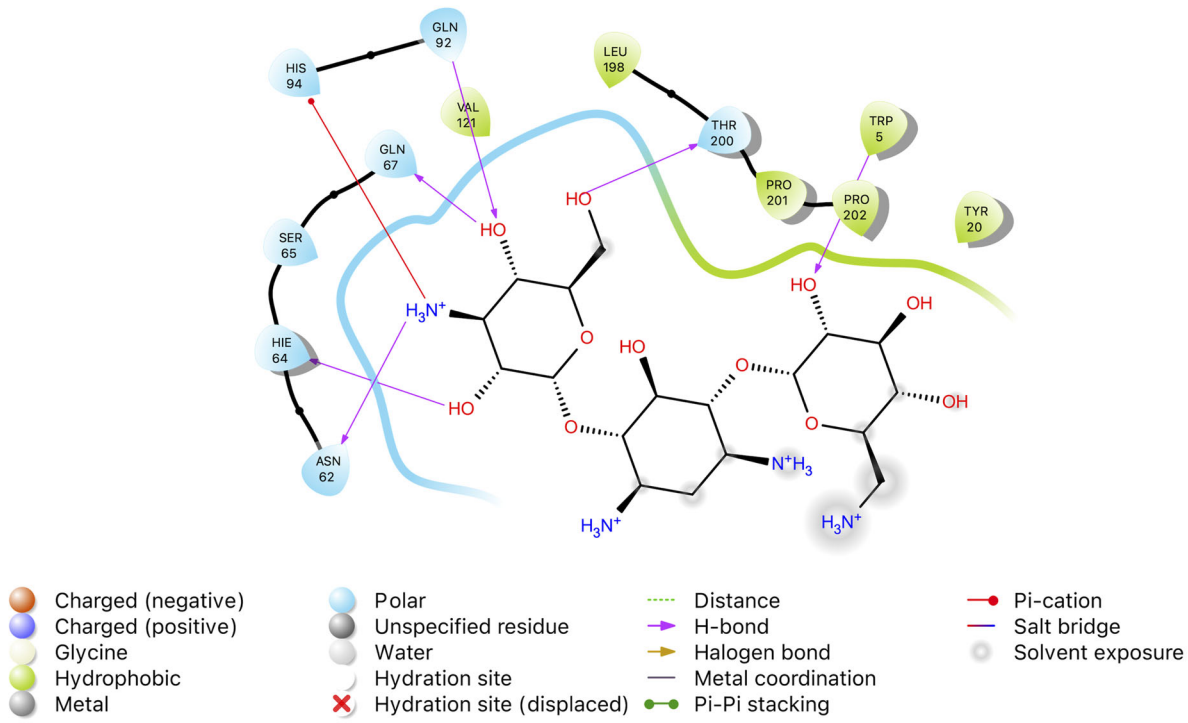

(B)

FIG 4 Molecular docking of *h*CA VII (PDB ID: 6H37) with kanamycin. (A) 3D ligand interaction diagram of 6H37 with kanamycin. (B) 2D docking pose of kanamycin with the key amino acids within the binding pocket of 6H37

1.86 Å) and Thr200 (distance 2.29 Å) from the binding site residues of *h*CA VII. Moreover, lincomycin was supported by hydrophobic residues: Trp5, Val121, Phe131, Ala135, Leu141, Leu198, Pro201, and Pro202 (Figure 5).

4 | CONCLUSIONS

Today, a new era is approaching because of the increase in the level of knowledge in the field of medicine,

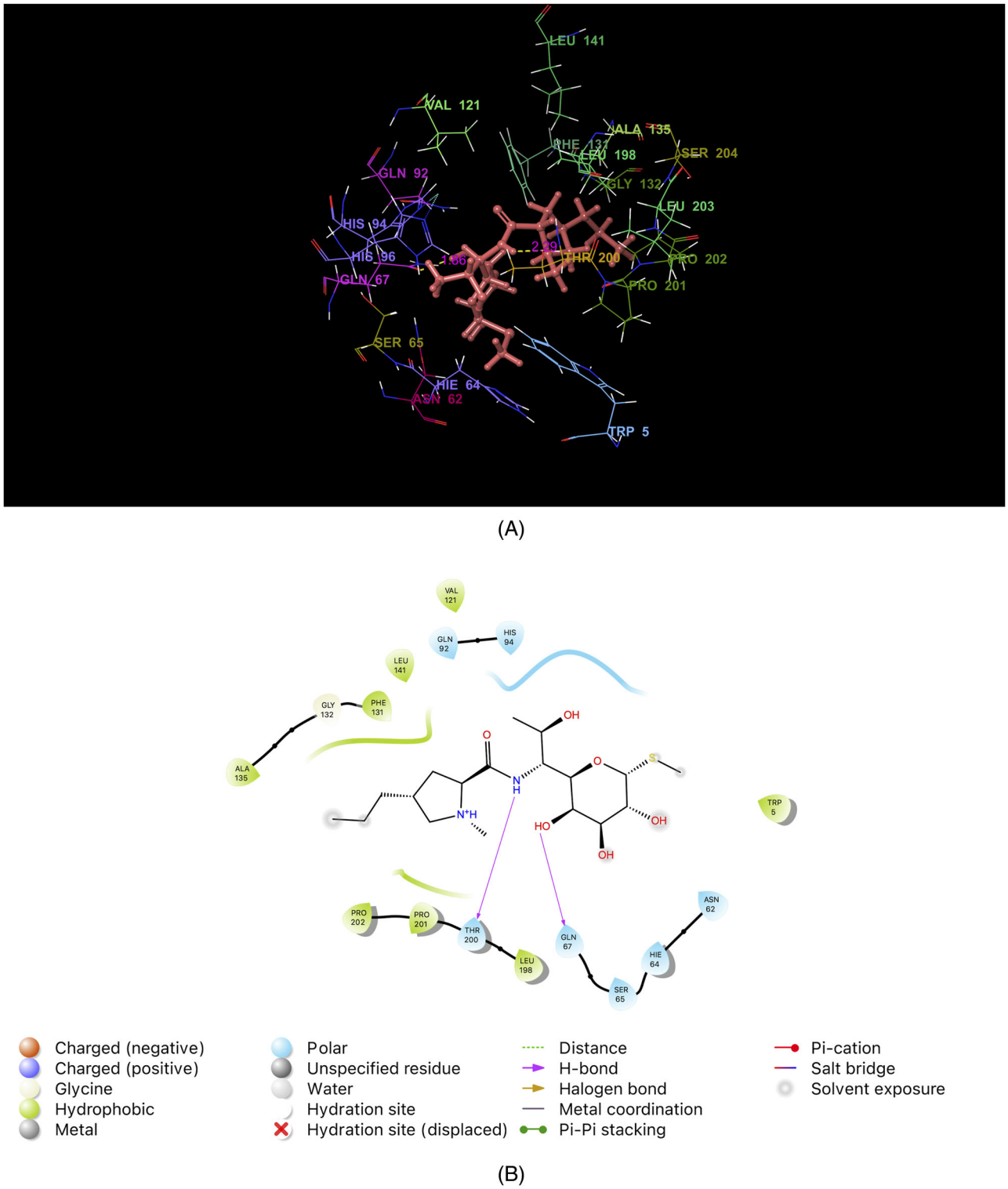

FIG 5 Molecular docking of *h*CA VII (PDB ID: 6H37) with lincomycin HCl. (A) 3D ligand interaction diagram of 6H37 with lincomycin. (B) 2D docking pose of lincomycin HCl with the key amino acids within the binding pocket of 6H37

genetics, and proteins, in terms of solving the mechanisms of various diseases and making the correct diagnosis and necessary treatment approaches. Therefore, many human proteins such as antibodies, vaccines, natural interferons, and various metabolic enzymes, which are used to diagnose and treat many diseases, have been recombinantly produced. In this study, which aims to produce a fast and simple method for recombinant production of hCA VII enzyme and to understand the biochemical behavior of this enzyme against therapeutics, inhibition effects of

commonly used antibiotics against rhCA VII was investigated. The K_I values were found between 0.29 μM and 157.6 mM. Finally, to further understand the binding interactions on the active site of this recombinant enzyme, molecular docking investigations of these antibiotics were undertaken. These results will help us identify new therapeutic strategies for drug design and discovery. In the following years, the recombinant products produced by the development of this technology will also be combined with other small molecules that may have a synergistic effect.

ACKNOWLEDGMENT

This work was supported by the Research Fund of Anadolu University under grant number 2102S003.

CONFLICT OF INTEREST

The authors declare that there is no conflict of interest.

ORCID

Hatice Esra Duran https://orcid.org/0000-0003-2080-0091
Şükrü Beydemir https://orcid.org/0000-0003-3667-6902

REFERENCES

1. Leader B, Baca QJ, Golan DE. Protein therapeutics: a summary and pharmacological classification. Nat Rev Drug Discov. 2008;7:21–39. https://doi.org/10.1038/nrd2399
2. Maheshwari N, Kumar M, Thakur IS, Srivastava S. Cloning, expression and characterization of β-and γ-carbonic anhydrase from Bacillus sp. SS105 for biomimetic sequestration of CO_2. Int J Biol Macromol. 2019;131:445–52. https://doi.org/10.1016/j.ijbiomac.2019.03.082
3. Boztas M, Cetinkaya Y, Topal M, Gulcin I, Menzek A, Sahin E, et al. Synthesis and carbonic anhydrase isoenzymes I, II, IX, and XII inhibitory effects of dimethoxybromophenol derivatives incorporating cyclopropane moieties. J Med Chem. 2015;58:640–50. https://doi.org/10.1021/jm501573b
4. Bilginer S, Gul HI, Anil B, Demir Y, Gulcin I. Synthesis and in silico studies of triazene-substituted sulfamerazine derivatives as acetylcholinesterase and carbonic anhydrases inhibitors. Arch Pharm (Weinheim). 2021;354:2000243. https://doi.org/10.1002/ardp.202000243
5. Demir Y, Oruç E, Topal A. Carbonic anhydrase activity responses and histopathological changes in gill and liver tissues after acute exposure to chromium in brown trout juveniles. Hacettepe J Biol Chem. 2016;44:515–23. https://doi.org/10.15671/HJBC.2016.132
6. Askin S, Tahtaci H, Türkeş C, Demir Y, Ece A, Çiftçi GA, et al. Design, synthesis, characterization, in vitro and in silico evaluation of novel imidazo [2, 1-b]1, 3, 4 thiadiazoles as highly potent acetylcholinesterase and non-classical carbonic anhydrase inhibitors. Bioorg Chem. 2021;113:105009. https://doi.org/10.1016/j.bioorg.2021.105009
7. Burmaoglu S, Yilmaz AO, Polat MF, Kaya R, Gulcin İ, Algul O. Synthesis and biological evaluation of novel tris-chalcones as potent carbonic anhydrase, acetylcholinesterase, butyrylcholinesterase and α-glycosidase inhibitors. Bioorg Chem. 2019;85:191–7. https://doi.org/10.1016/j.bioorg.2018.12.035
8. Supuran CT. Advances in structure-based drug discovery of carbonic anhydrase inhibitors. Expert Opin Drug Discovery. 2017;12:61–88. https://doi.org/10.1080/17460441.2017.1253677
9. Tugrak M, Gul HI, Demir Y, Gulcin I. Synthesis of benzamide derivatives with thiourea-substituted benzenesulfonamides as carbonic anhydrase inhibitors. Arch Pharm (Weinheim). 2020;354:e2000230. https://doi.org/10.1002/ardp.202000230
10. Huyut Z, Beydemir Ş, Gülçin İ. Inhibition properties of some flavonoids on carbonic anhydrase I and II isoenzymes purified from human erythrocytes. J Biochem Mol Toxicol. 2017;31:e21930. https://doi.org/10.1002/jbt.21930
11. Balseven H, İşgör MM, Mert S, Alım Z, Beydemir Ş, Ok S, et al. Facile synthesis and characterization of novel pyrazole-sulfonamides and their inhibition effects on human carbonic anhydrase isoenzymes. Bioorg Med Chem. 2013;21:21–7. https://doi.org/10.1016/j.bmc.2012.11.012
12. Garibov E, Taslimi P, Sujayev A, Bingol Z, Çetinkaya S, Gulçin İ, et al. Synthesis of 4, 5-disubstituted-2-thioxo-1, 2, 3, 4-tetrahydropyrimidines and investigation of their acetylcholinesterase, butyrylcholinesterase, carbonic anhydrase I/II inhibitory and antioxidant activities. J Enzyme Inhib Med Chem. 2016;31:1–9. https://doi.org/10.1080/14756366.2016.1198901
13. Mert S, Alım Z, İşgör MM, Beydemir Ş, Kasımoğulları R. The synthesis of novel pyrazole-3, 4-dicarboxamides bearing 5-amino-1, 3, 4-thiadiazole-2-sulfonamide moiety with effective inhibitory activity against the isoforms of human cytosolic carbonic anhydrase I and II. Bioorg Chem. 2016;68:64–71. https://doi.org/10.1016/j.bioorg.2016.07.006
14. Angeli A, Tanini D, Capperucci A, Supuran CT. First evaluation of organotellurium derivatives as carbonic anhydrase I, II, IV, VII and IX inhibitors. Bioorg Chem. 2018;76:268–72. https://doi.org/10.1016/j.bioorg.2017.12.010
15. Aslan HE, Demir Y, Özaslan MS, Türkan F, Beydemir Ş, Küfrevioğlu ÖI. The behavior of some chalcones on acetylcholinesterase and carbonic anhydrase activity. Drug Chem Toxicol. 2019;42:634–40. https://doi.org/10.1080/01480545.2018.1463242
16. Neumann JT, Tzikas S, Funke-Kaiser A, Wilde S, Appelbaum S, Keller T, et al. Association of MR-proadrenomedullin with cardiovascular risk factors and subclinical cardiovascular disease. Atherosclerosis. 2013;228:451–9. https://doi.org/10.1016/j.atherosclerosis.2013.03.006
17. Thiry A, Masereel B, Dogné JM, Supuran CT, Wouters J, Michaux C. Exploration of the binding mode of indanesulfonamides as selective inhibitors of human carbonic anhydrase type VII by targeting Lys 91. ChemMedChem. 2007;2:1273–80. https://doi.org/10.1002/cmdc.200700057
18. Truppo E, Supuran CT, Sandomenico A, Vullo D, Innocenti A, Di Fiore A, et al. Carbonic anhydrase VII is S-glutathionylated without loss of catalytic activity and affinity for sulfonamide inhibitors. Bioorg Med Chem Lett. 2012;22:1560–4. https://doi.org/10.1016/j.bmcl.2011.12.134
19. Yan Z, Yang Q, Wang X, Torres OL, Tang S, Zhang S, et al. Correlation between antibiotic-induced feeding depression and body size reduction in zooplankton (rotifer, Brachionus calyciflorus):

neural response and digestive enzyme inhibition. Chemosphere. 2019;218:376–83. https://doi.org/10.1016/j.chemosphere.2018.11.067
20. Oliveira MT, Moura GM, da Cruz JIO, Lima RVC, Santos EAD, et al. Serine protease inhibition and modulatory-antibiotic activity of the proteic extract and fractions from *Amburana cearensis*. Food Chem Toxicol. 2020;135:110946
21. Ketha H, Garg U. Toxicology cases for the clinical and forensic laboratory, Academic Press, 2020;
22. Bradford N. A rapid and sensitive method for the quantitation of microgram quantities of protein utilizing the principle of protein-dye binding. Anal Biochem. 1976;72:248–54. https://doi.org/10.1016/0003-2697(76)90527-3
23. Türkeş C, Söyüt H, Beydemir Ş. Effect of calcium channel blockers on paraoxonase-1 (PON1) activity and oxidative stress. Pharmacol Rep. 2014;66:74–80. https://doi.org/10.1016/j.pharep.2013.08.007
24. Demir Y, Taslimi P, Koçyiğit ÜM, Akkuş M, Özaslan MS, Duran HE, et al. Determination of the inhibition profiles of pyrazolyl–thiazole derivatives against aldose reductase and α-glycosidase and molecular docking studies. Arch Pharm (Weinheim). 2020;353:2000118. https://doi.org/10.1002/ardp.202000118
25. Laemmli UK. Cleavage of structural proteins during the assembly of the head of bacteriophage T4. Nature. 1970;227:680–5. https://doi.org/10.1038/227680a0
26. Türkeş C, Söyüt H, Beydemir Ş. Human serum paraoxonase-1 (hPON1): in vitro inhibition effects of moxifloxacin hydrochloride, levofloxacin hemihidrate, cefepime hydrochloride, cefotaxime sodium and ceftizoxime sodium. J Enzyme Inhib Med Chem. 2015;30:622–8. https://doi.org/10.3109/14756366.2014.959511
27. Demir Y. The behaviour of some antihypertension drugs on human serum paraoxonase-1: an important protector enzyme against atherosclerosis. J Pharm Pharmacol. 2019;71:1576–83. https://doi.org/10.1111/jphp.13144
28. Verpoorte JA, Mehta S, Edsall JT. Esterase activities of human carbonic anhydrases B and C. J Biol Chem. 1967;242:4221–9. https://doi.org/10.1016/S0021-9258(18)95800-X
29. Sever B, Türkeş C, Altıntop MD, Demir Y, Beydemir Ş. Thiazolyl-pyrazoline derivatives: in vitro and in silico evaluation as potential acetylcholinesterase and carbonic anhydrase inhibitors. Int J Biol Macromol. 2020;163:1970–88. https://doi.org/10.1016/j.ijbiomac.2020.09.043
30. Aslan HE, Beydemir Ş. Phenolic compounds: the inhibition effect on polyol pathway enzymes. Chem Biol Interact. 2017;266:47–55. https://doi.org/10.1016/j.cbi.2017.01.021
31. Demir Y, Duran HE, Durmaz L, Taslimi P, Beydemir Ş, Gulcin I. The influence of some nonsteroidal anti-inflammatory drugs on metabolic enzymes of aldose reductase, sorbitol dehydrogenase, and α-glycosidase: a perspective for metabolic disorders. Appl Biochem Biotechnol. 2020;190:437–47. https://doi.org/10.1007/s12010-019-03099-7
32. Özaslan MS, Demir Y, Aslan HE, Beydemir Ş, Küfrevioğlu Öİ. Evaluation of chalcones as inhibitors of glutathione S-transferase. J Biochem Mol Toxicol. 2018;32:e22047. https://doi.org/10.1002/jbt.22047
33. Türkeş C, Demir Y, Beydemir Ş. Anti-diabetic properties of calcium channel blockers: inhibition effects on aldose reductase enzyme activity. Appl Biochem Biotechnol. 2019;189:318–29. https://doi.org/10.1007/s12010-019-03009-x
34. Caglayan C, Taslimi P, Türk C, Gulcin I, Kandemir FM, Demir Y, et al. Inhibition effects of some pesticides and heavy metals on carbonic anhydrase enzyme activity purified from horse mackerel (*Trachurus trachurus*) gill tissues. Environ Sci Pollut Res Int. 2020;28(10):10607–16. https://doi.org/10.1007/s11356-020-07611-z
35. Akbaba Y, Türkeş C, Polat L, Söyüt H, Şahin E, Menzek A, et al. Synthesis and paroxonase activities of novel bromophenols. J Enzyme Inhib Med Chem. 2013;28:1073–9. https://doi.org/10.3109/14756366.2012.715287
36. Yaşar Ü, Gönül İ, Türkeş C, Demir Y, Beydemir Ş. Transition-metal complexes of bidentate Schiff-base ligands: in vitro and in silico evaluation as non-classical carbonic anhydrase and potential acetylcholinesterase inhibitors. ChemistrySelect. 2021;6:7278–84. https://doi.org/10.1002/slct.202102082
37. Lineweaver H, Burk D. The determination of enzyme dissociation constants. J Am Chem Soc. 1934;56:658–66. https://doi.org/10.1021/ja01318a036
38. Akocak S, Taslimi P, Lolak N, Işık M, Durgun M, Budak Y, et al. Synthesis, characterization, and inhibition study of novel substituted phenylureido sulfaguanidine derivatives as α-glycosidase and cholinesterase inhibitors. Chem Biodivers. 2021;18:e2000958. https://doi.org/10.1002/cbdv.202000958
39. Türkeş C, Söyüt H, Beydemir Ş. Inhibition effects of gemcitabine hydrochloride, acyclovir, and 5-fluorouracil on human serum paraoxonase-1 (hPON1): in vitro. Open J Biochem. 2013;1:10–5. https://doi.org/10.15764/BIOC.2014.01002
40. Demir Y. Naphthoquinones, benzoquinones, and anthraquinones: molecular docking, ADME and inhibition studies on human serum paraoxonase-1 associated with cardiovascular diseases. Drug Dev Res. 2020;81:628–36. https://doi.org/10.1002/ddr.21667
41. Türkeş C, Söyüt H, Beydemir Ş. In vitro inhibitory effects of palonosetron hydrochloride, bevacizumab and cyclophosphamide on purified paraoxonase-I (hPON1) from human serum. Environ Toxicol Pharmacol. 2016;42:252–7. https://doi.org/10.1016/j.etap.2015.11.024
42. Sever B, Altıntop MD, Demir Y, Türkeş C, Özbaş K, Çiftçi GA, et al. A new series of 2,4-thiazolidinediones endowed with potent aldose reductase inhibitory activity. Open Chem. 2021;19:347–57. https://doi.org/10.1515/chem-2021-0032
43. Demir Y, Türkeş C, Beydemir Ş. Molecular docking studies and inhibition properties of some antineoplastic agents against paraoxonase-I. Anticancer Agents Med Chem. 2020;20:887–96. https://doi.org/10.2174/1871520620666200218110645
44. Işık M, Demir Y, Durgun M, Türkeş C, Necip A, Beydemir Ş. Molecular docking and investigation of 4-(benzylideneamino)- and 4-(benzylamino)-benzenesulfonamide derivatives as potent AChE inhibitors. Chem Pap. 2020;74:1395–405. https://doi.org/10.1007/s11696-019-00988-3
45. Türkeş C. A potential risk factor for paraoxonase 1: in silico and in-vitro analysis of the biological activity of proton-pump inhibitors. J Pharm Pharmacol. 2019;71:1553–64. https://doi.org/10.1111/jphp.13141
46. Durgun M, Türkeş C, Işık M, Demir Y, Saklı A, Kuru A, et al. Synthesis, characterization, biological evaluation and in silico

studies of sulfonamide Schiff bases. J Enzyme Inhib Med Chem. 2020;35:950–62. https://doi.org/10.1080/14756366.2020.1746784
47. Türkeş C, Arslan M, Demir Y, Cocaj L, Nixha AR, Beydemir Ş. Synthesis, biological evaluation and in silico studies of novel N-substituted phthalazine sulfonamide compounds as potent carbonic anhydrase and acetylcholinesterase inhibitors. Bioorg Chem. 2019;89:103004. https://doi.org/10.1016/j.bioorg.2019.103004
48. Gündoğdu S, Türkeş C, Arslan M, Demir Y, Beydemir Ş. New isoindole-1, 3-dione substituted sulfonamides as potent inhibitors of carbonic anhydrase and acetylcholinesterase: design, synthesis, and biological evaluation. ChemistrySelect. 2019;4:13347–55. https://doi.org/10.1002/slct.201903458
49. Buemi MR, Di Fiore A, De Luca L, Angeli A, Mancuso F, Ferro S, et al. Exploring structural properties of potent human carbonic anhydrase inhibitors bearing a 4-(cycloalkylamino-1-carbonyl) benzenesulfonamide moiety. Eur J Med Chem. 2019;163:443–52. https://doi.org/10.1016/j.ejmech.2018.11.073
50. Türkeş C, Beydemir Ş. Inhibition of human serum paraoxonase-I with antimycotic drugs: in vitro and in silico studies. Appl Biochem Biotechnol. 2020;190:252–69. https://doi.org/10.1007/s12010-019-03073-3
51. Işık M, Akocak S, Lolak N, Taslimi P, Türkeş C, Gülçin İ, et al. Synthesis, characterization, biological evaluation, and in silico studies of novel 1,3-diaryltriazene-substituted sulfathiazole derivatives. Arch Pharm (Weinheim). 2020;353:e2000102. https://doi.org/10.1002/ardp.202000102
52. Lolak N, Akocak S, Türkeş C, Taslimi P, Işık M, Beydemir Ş, et al. Synthesis, characterization, inhibition effects, and molecular docking studies as acetylcholinesterase, α-glycosidase, and carbonic anhydrase inhibitors of novel benzenesulfonamides incorporating 1,3,5-triazine structural motifs. Bioorg Chem. 2020;100:103897. https://doi.org/10.1016/j.bioorg.2020.103897
53. Güleç Ö, Türkeş C, Arslan M, Demir Y, Yeni Y, Hacımüftüoğlu A, et al. Cytotoxic effect, enzyme inhibition, and in silico studies of some novel N-substituted sulfonyl amides incorporating 1, 3, 4-oxadiazol structural motif. Mol Divers. 2022:1–21. https://doi.org/10.1007/s11030-022-10422-8
54. Harder E, Damm W, Maple J, Wu C, Reboul M, Xiang JY, et al. OPLS3: a force field providing broad coverage of drug-like small molecules and proteins. J Chem Theory Comput. 2016;12:281–96. https://doi.org/10.1021/acs.jctc.5b00864
55. Demir Y, Ceylan H, Türkeş C, Beydemir Ş. Molecular docking and inhibition studies of vulpinic, carnosic and usnic acids on polyol pathway enzymes. J Biomol Struct Dyn. 2021:1–14. https://doi.org/10.1080/07391102.2021.1967195
56. Kilic A, Beyazsakal L, Işık M, Türkeş C, Necip A, Takım K, et al. Mannich reaction derived novel boron complexes with amine-bis(phenolate) ligands: synthesis, spectroscopy and in vitro/in silico biological studies. J Organomet Chem. 2020;927:121542. https://doi.org/10.1016/j.jorganchem.2020.121542
57. Türkeş C, Akocak S, Işık M, Lolak N, Taslimi P, Durgun M, et al. Novel inhibitors with sulfamethazine backbone: synthesis and biological study of multi-target cholinesterases and α-glucosidase inhibitors. J Biomol Struct Dyn. 2021:1–13. https://doi.org/10.1080/07391102.2021.1916599
58. Türkeş C, Beydemir Ş, Küfrevioğlu Öİ. In vitro and in silico studies on the toxic effects of antibacterial drugs as human serum paraoxonase 1 inhibitor. ChemistrySelect. 2019;4:9731–6. https://doi.org/10.1002/slct.201902424
59. Çalışkan B, Demir Y, Türkeş C. Ophthalmic drugs: in vitro paraoxonase 1 inhibition and molecular docking studies. Biotechnol Appl Biochem. 2021;1–11. https://doi.org/10.1002/bab.2284
60. Işık M, Beydemir Ş, Demir Y, Durgun M, Türkeş C, Nasır A, et al. Benzenesulfonamide derivatives containing imine and amine groups: inhibition on human paraoxonase and molecular docking studies. Int J Biol Macromol. 2020;146:1111–23. https://doi.org/10.1016/j.ijbiomac.2019.09.237
61. Türkeş C, Demir Y, Beydemir Ş. calcium channel blockers: molecular docking and inhibition studies on carbonic anhydrase I and II isoenzymes. J Biomol Struct Dyn. 2021;39:1672–80. https://doi.org/10.1080/07391102.2020.1736631
62. Türkeş C, Demir Y, Beydemir Ş. Some calcium-channel blockers: kinetic and in silico studies on paraoxonase-I. J Biomol Struct Dyn. 2020;40:77–85. https://doi.org/10.1080/07391102.2020.1806927
63. Tokalı FS, Demir Y, Demircioğlu İH, Türkeş C, Kalay E, Şendil K, et al. Synthesis, biological evaluation, and in silico study of novel library sulfonates containing quinazolin-4 (3H)-one derivatives as potential aldose reductase inhibitors. Drug Dev Res. 2022;83(3):586–604. https://doi.org/10.1002/ddr.21887
64. Beydemir Ş, Türkeş C, Yalçın A. Gadolinium-based contrast agents: in vitro paraoxonase 1 inhibition, in silico studies. Drug Chem Toxicol. 2021;44:508–17. https://doi.org/10.1080/01480545.2019.1620266
65. Türkeş C. Inhibition effects of phenolic compounds on human serum paraoxonase-1 enzyme. J Inst Sci Tech. 2019;9:1013–22. https://doi.org/10.21597/jist.491054
66. Osmaniye D, Türkeş C, Demir Y, Özkay Y, Beydemir Ş, Kaplancıklı ZA. Design, synthesis, and biological activity of novel dithiocarbamate-methylsulfonyl hybrids as carbonic anhydrase inhibitors. Arch Pharm (Weinheim). 2022;355:e2200132. https://doi.org/10.1002/ardp.202200132
67. Türkeş C. Investigation of potential paraoxonase-I inhibitors by kinetic and molecular docking studies: chemotherapeutic drugs. Protein Pept Lett. 2019;26:392–402. https://doi.org/10.2174/0929866526666190226162225
68. Friesner RA, Murphy RB, Repasky MP, Frye LL, Greenwood JR, Halgren TA, et al. Extra precision glide: docking and scoring incorporating a model of hydrophobic enclosure for protein−ligand complexes. J Med Chem. 2006;49:6177–96. https://doi.org/10.1021/jm051256o
69. Yapar G, Duran HE, Lolak N, Akocak S, Türkeş C, Durgun M, et al. Biological effects of bis-hydrazone compounds bearing isovanillin moiety on the aldose reductase. Bioorg Chem. 2021;117:105473. https://doi.org/10.1016/j.bioorg.2021.105473
70. Istrefi Q, Türkeş C, Arslan M, Demir Y, Nixha AR, Beydemir Ş, et al. Sulfonamides incorporating ketene N,S-acetal bioisosteres as potent carbonic anhydrase and acetylcholinesterase inhibitors. Arch Pharm (Weinheim). 2020;353:e1900383. https://doi.org/10.1002/ardp.201900383
71. Taslimi P, Işık M, Türkan F, Durgun M, Türkeş C, Gülçin İ, et al. Benzenesulfonamide derivatives as potent acetylcholinesterase, α-glycosidase, and glutathione S-transferase inhibitors: biological evaluation and molecular docking studies. J Biomol

Struct Dyn. 2020;39:5449–60. https://doi.org/10.1080/07391102.2020.1790422
72. Türkeş C, Kesebir Öztürk A, Demir Y, Küfrevioğlu Öİ, Beydemir Ş. Calcium channel blockers: the effect of glutathione S-transferase enzyme activity and molecular docking studies. ChemistrySelect. 2021;6:11137–43. https://doi.org/10.1002/slct.202103100
73. Kalaycı M, Türkeş C, Arslan M, Demir Y, Beydemir Ş. Novel benzoic acid derivatives: synthesis and biological evaluation as multi-target acetylcholinesterase and carbonic anhydrase inhibitors. Arch Pharm (Weinheim). 2021;354:e2000282. https://doi.org/10.1002/ardp.202000282
74. Sever B, Türkeş C, Altıntop MD, Demir Y, Çiftçi GA, Beydemir Ş. Novel metabolic enzyme inhibitors designed through the molecular hybridization of thiazole and pyrazoline scaffolds. Arch Pharm (Weinheim). 2021;354:e2100294. https://doi.org/10.1002/ardp.202100294
75. Türkeş C, Demir Y, Beydemir Ş. Infection medications: assessment in-vitro glutathione S-transferase inhibition and molecular docking study. ChemistrySelect. 2021;6:11915–24. https://doi.org/10.1002/slct.202103197
76. Khan S, Ullah MW, Siddique R, Nabi G, Manan S, Yousaf M, et al. Role of recombinant DNA technology to improve life. Int J Genomics. 2016;2016:2405954. https://doi.org/10.1155/2016/2405954
77. Demir Y, Beydemir Ş. Purification, refolding, and characterization of recombinant human paraoxonase-1. Turk J Chem. 2015;39:764–76. https://doi.org/10.3906/kim-1501-51
78. Boggio R, Colombo R, Hay RT, Draetta GF, Chiocca S. A mechanism for inhibiting the SUMO pathway. Mol Cell. 2004;16:549–61. https://doi.org/10.1016/j.molcel.2004.11.007
79. Wang Z, Li H, Guan W, Ling H, Wang Z, Mu T, et al. Human SUMO fusion systems enhance protein expression and solubility. Protein Expr Purif. 2010;73:203–8. https://doi.org/10.1016/j.pep.2010.05.001
80. Schilling CH, Letscher D, Palsson BØ. Theory for the systemic definition of metabolic pathways and their use in interpreting metabolic function from a pathway-oriented perspective. J Theor Biol. 2000;203:229–48. https://doi.org/10.1006/jtbi.2000.1073
81. Erdemir F, Celepci DB, Aktaş A, Gök Y, Kaya R, Taslimi P, et al. Novel 2-aminopyridine liganded Pd (II) N-heterocyclic carbene complexes: synthesis, characterization, crystal structure and bioactivity properties. Bioorg Chem. 2019;91:103134. https://doi.org/10.1016/j.bioorg.2019.103134
82. Ekinci D, Beydemir Ş. Evaluation of the impacts of antibiotic drugs on PON 1; a major bioscavenger against cardiovascular diseases. Eur J Pharmacol. 2009;617:84–9. https://doi.org/10.1016/j.ejphar.2009.06.048
83. Ekinci D, Beydemir S, Alim Z. Some drugs inhibit in vitro hydratase and esterase activities of human carbonic anhydrase-I and II. Pharmacol Rep. 2007;59:580.
84. Şengül B, Beydemir Ş. The interactions of cephalosporins on polyol pathway enzymes from sheep kidney. Arch Physiol Biochem. 2018;124:35–44. https://doi.org/10.1080/13813455.2017.1358749
85. Demir Y, Şengül B, Ergun B, Beydemir Ş. Alcohol dehydrogenase from sheep liver: purifcation, characterization and impacts of some antibiotics. J Inst Sci Technol. 2017;7:151–60.

SUPPORTING INFORMATION

Additional supporting information can be found online in the Supporting Information section at the end of this article.

How to cite this article: Duran HE, Beydemir Ş. Recombinant human carbonic anhydrase VII: Purification, characterization, inhibition, and molecular docking studies. Biotechnol Appl Biochem. 2023;70:415–428. https://doi.org/10.1002/bab.2367